Technical note

Artefactual time-course correlations in echo-planar fMRI with implications for studies of brain function

Nikolaus Kriegeskorte[1], Jerzy Bodurka[1,2] and Peter Bandettini[1,2]

[1]Section on Functional Imaging Methods, Laboratory of Brain and Cognition, National Institute of Mental Health, Bethesda, MD, USA

[2]Functional MRI Core Facility, National Institute of Mental Health, Bethesda, MD, USA

Running title: Artefactual fMRI correlations

Abstract

Background. Brain function is widely investigated with functional magnetic resonance imaging (fMRI) in humans and animals. In fMRI, the time courses of voxels typically reflect the local blood-oxygen level, which is taken as an indicator of neuronal activity. Voxel time-course correlations are often explicitly modeled and interpreted in terms of neuronal interactions. They also affect standard analyses that do not explicitly target neuronal interactions. As a consequence, time-course correlations between voxels influence conclusions about cognitive and physiological brain processes in many studies. However, voxel correlations are known to arise not only from cognitive and physiological processes, but also as artefacts of fMRI techniques such as the commonly used echoplanar imaging (EPI).

Methods and principal findings. We empirically demonstrate this phenomenon by plotting time-course correlation as a function of voxel separation for a human brain in resting state and for a water-filled sphere (called a "phantom"). The phantom served as a test object known not to contain any interacting neuronal systems. The plots for brain and phantom are surprisingly similar. The correlational structure found in the phantom must be artefactual. Artefactual correlations spanning many centimeters occur within and between different imaging slices.

Conclusions. Correlations between voxel time courses do not necessarily reflect brain processes. Instead, fMRI is affected by artefactual correlations, which are very strong for neighboring voxels and clearly present even at large distances. This needs to be taken into account in the neuroscientific interpretation of voxel correlations.

Introduction

In functional magnetic resonance imaging (fMRI) of brain activity, the time courses of voxels reflect the local blood-oxygen level, which is taken as an indicator of neuronal activity. Consequently, voxel time-course correlations are often explicitly modeled and interpreted in terms of neuronal interactions. This is the case in analyses of functional and effective connectivity (e.g. Friston et al. 1993; Büchel et al. 1997, McIntosh et al. 1998; Roebroeck et al. 2005) and regional time-course homogeneity (Zang et al. 2004, Goelman 2004). Voxel correlations are central also to principal- (e.g. Friston et al. 1993) and independent-component analyses (e.g. McKeown et al 1998, Formisano et al. 2004), which provide an alternative, more holistic and data-driven analysis of connectivity. Beyond connectivity studies, most other fMRI analyses are also indirectly affected by correlations between voxel time courses. For example, they affect multivariate analyses of activity-pattern information (e.g. Haxby et al. 2001, Cox and Savoy 2003, Kriegeskorte et al. 2006). Even in univariate contrast mapping, the significance threshold is usually a function of the statistical dependency between voxels (e.g. Worsley et al. 1992; Friston et al. 1994).

As a consequence, time-course correlations between voxels affect conclusions about cognitive and physiological brain processes in many studies. However, voxel correlations are known to arise not only from cognitive and physiological processes, but also as artefacts of fMRI techniques such as the commonly used echoplanar imaging (EPI).

When a time-course correlation between two brain regions is shown to change across experimental conditions, this does suggest changes in the neuronal interaction between the regions (assuming that any artefactual component is unaffected by experimental condition and overall activity level). Nevertheless it is important to be aware of the artefactual component and a better characterization of it is desirable.

In this note, we demonstrate the phenomenon by plotting time-course correlation as a function of voxel separation for a human brain in resting state and for an MRI phantom (a water-filled sphere). The two plots are surprisingly similar given that any correlational structure found in the phantom must be artefactual. Artefactual correlations spanning many centimeters occur within and between different imaging slices. This phenomenon may deserve more attention at the level of (1) fMRI pulse-sequence design, (2) statistical analysis techniques, and (3) the interpretation of analysis results in terms of brain function.

Methods

Rationale

We study time-course correlation for pairs of voxels as a function of (1) the type of object measured (human brain or MRI water phantom), (2) the distance between the two voxels, (3) the orientation of the voxel pair relative to the EPI acquisition slab (readout, phase-encoding, slice-selection), and (4) the location of the voxel pair in the volume (e.g. inside or outside the object measured).

We plot the correlation coefficients as a function of the distance between voxels (see Figs. 1 and 2). Furthermore we compute neighbor-correlation maps (Fig. 3). For a given shift vector between voxels, each such map shows the continuous variation of pairwise voxel correlations across space.

Measurement details

A General Electric Signa VH 3-Tesla MRI scanner was used for EPI. For signal reception, the standard head transmit/receive RF coil was used. Following conventional practice, the first 4 scan volumes were omitted from the analysis.

Human data. A human subject was scanned in resting state with eyes closed. The in-plane voxel size was $(3.125\ \text{mm})^2$. We acquired 8 axial slices of thickness 4 mm with a gap of 2 mm. The slice matrix was 64 by 64 with a field of view of 200 mm. The flip angle was 90 deg, TR: 3 s, TE: 45 ms. The number of volumes analyzed was 70.

Phantom data. The MRI phantom was a sphere filled with water. The in-plane voxel size was $(2.8125\ \text{mm})^2$. We acquired 8 coronal slices of thickness 4 mm with a gap of 1 mm. The slice matrix was 64 by 64 with a field of view of 180 mm. The flip angle was 90 deg, TR: 2 s, TE: 30 ms. The number of volumes analyzed was 70.

Results

We describe results for two particular data sets (human brain, phantom). However, we have observed similar results with different scanners and fMRI sequence parameters, including high-resolution fMRI data.

In Figs. 1 and 2, we used regions of interest to limit the number of pairwise correlations. However, the results we describe are not strongly dependent on the placement of the regions. Note also that Fig. 3 maps out voxel correlations without any spatial restriction.

Common findings for human brain and MRI phantom

High correlations for neighboring voxels

For both a human brain and an MRI phantom, EPI-based fMRI data exhibited substantial voxel-time-course correlations with the following properties: We found voxel pairs with

positive as well as voxel pairs with negative correlations. Between adjacent voxels the average correlation was positive and fell between 0.4 and 0.6 (linear correlation coefficient) for voxels inside the object (brain or phantom) in the same EPI slice. Between EPI slices correlations between adjacent voxels averaged around 0.2 (Fig. 1).

Quick-then-slow drop of average correlations with voxel separation
Average correlations quickly dropped to about 0.2 within the first few voxel widths (< 6 mm voxel-center separation, Fig. 1). Beyond 1 cm voxel separation, they continued to fall off, but very slowly, remaining clearly present even at a distances of several centimeters (Figs. 1 and 2). The average correlation appears roughly proportional to absolute signal intensity (not shown) and is, thus, close to zero outside the object (Fig. 1). Since these observations hold for a brain and an MRI phantom, a substantial portion of the correlations may be artefactual.

Different findings for human brain and MRI phantom

Phantom average correlations vanish at 8 cm voxel separation.
Phantom average correlations fell off to 0 about linearly within about 8 cm voxel separation (Fig. 2). This held for both within- and between-EPI-slice pairs of voxels. However, average correlations tended to be higher in the readout direction than either in the phase-encode direction or between EPI slices. Quantitatively, $r \approx 0.12$ for adjacent voxels across slices, $r \approx 0.15$ for the same distance within a slice along the phase-encode direction, and $r \approx 0.42$ for the same distance within a slice along the readout direction. Fig. 2 shows this for a range of distances. In the phase-encode direction the average correlation vanished at about 3 cm voxel separation.

Human-brain average voxel correlations remain positive even at long ranges.
In the human brain, average correlations did not vanish within the first 8 cm of voxel separation. Instead they appeared to asymptote at a positive correlation coefficient of about 0.1 (Fig. 2).

Correlations are more variable in the human brain than in the phantom.
The variability of correlation coefficients was found to be much greater in the human brain than in the phantom for ROIs inside as well as outside the object (Fig. 1). (In both phantom and brain, correlations inside the object were more variable than those outside the object.)

Discussion

We observed fMRI voxel time-course correlations not only when imaging an brain, but also for a phantom. This indicates that there is a contribution of the non-neuronal factors to fMRI voxel correlations. The possible factors causing these artefactual correlations, including physiological and instrumental factors, are summarized in Fig. 4.

What are the specific causes of the long-range correlations?

The presence of long-range spatial correlations in the phantom data may indicate a contribution of scanner instability and/or system noise. The presence of similar long-range correlations in human data is likely to reflect a combination of (1) these imaging-related factors, (2) physiological global signal correlations including those caused by respiration, and (3) the presence of correlated neuronal activity targeted by studies of functional and effective connectivity.

What are the specific causes of the short-range correlations?

One cause of short-range correlations is that image reconstruction from k-space data is associated with a sinc-function point spread of the energy of each pixel (Schmitt et al. 1998). In EPI with long readout windows (e.g. single-shot), there is an additional resolution loss in the phase-encoding direction due to the filter effect of the T2*-decay of the MRI signal (Schmitt et al. 1998; Farzaneh et al. 1990). However, we observe greater correlations between voxels adjacent along the readout than the phase-encoding direction, suggesting that this latter source of correlation does not dominate in our data.

Could mechanical vibration and head motion play a role?

Subject head motion can lead to correlations and anti-correlations of voxel time courses even at opposite sides of the head (i.e. at long range). In addition to this kind of intrinsic motion, which is absent for a phantom, any object subjected to fMRI will be affected to some extent by mechanical vibration from the gradient system. Mechanical vibration, in principle, could cause coherent oscillatory displacement and could, thus, be a factor in the causation of the voxel time-course correlations we observed. However, we would like to add a few critical thoughts on this explanation.

The mechanical properties of a phantom and a human head are very different. In particular, the brain is embedded in cerebral spinal fluid (CSF). One of the biological functions of CSF is to reduce the brain's exposure to mechanical vibration and trauma from the outside world. Since the mechanical properties of phantom matter (water) are much more uniform than those of the human brain (gray matter, white matter, and CSF all them have different mechanical properties, such as viscosity), one might expect very different results for these two scenarios if mechanical vibration was the major cause of voxel correlation. Moreover, the mechanical isolation of the phantom and human brain from the magnet table and RF coil, both conducting mechanical vibration from the gradients, were very different.

Could interactions among water molecules play a role?

We think that the effects of molecular water diffusion during our experimental echo time must be negligible. They can be estimated based on Einstein's (1956) equation for diffusion length or displacement (Δx) derived to describe random thermally-induced Brownian motion. For simplicity, we assume non-restrictive diffusion in three dimensions. The equation for mean square displacement is: $\Delta x^2 = 6\ D\ TE$ (Einstein 1956),

where D is water diffusion coefficient, which at room temperature is on the order of 10^{-9} m^2/s (Fick 1855), and TE is the echo time. This gives a Δx equal to 16.4 10^{-6} m for TE=45 ms. At voxel widths of 3-4 mm, as here, water molecule displacement during the TE is about 190 times smaller than voxel width. In order for Δx to be comparable to the voxel width, say about 1 mm, the diffusion coefficient would have to be more than three orders of magnitude larger than 10^{-9} m^2/s. Even if water diffusion were restricted and non-Gaussian, such as in the human eye lens (the highest concentration of the protein in the human body), resulting in a modification of the equation (Bodurka 1997), a very unrealistic value of the water diffusion coefficient would be required to produce displacements on the order of the fMRI voxel width used here (Crank 1975).

In sum, water diffusion can only have negligible effects on correlations between voxels. This should hold even when the voxels are quite close together in the volume. Note, however, that we observed correlations even over long ranges in space.

To what extent are the correlations found in the human brain artefactual?

Our results show that substantial artefactual correlations do arise from non-neuronal factors. The artefactual covariance seen for the phantom can be expected to be present in the human data as well. However, the fact that there is some similarity between human and phantom data does not imply that all or most of the covariance seen in the human is artefactual. If genuine physiological and cognitive covarying signals added to the artefactually covarying noise have a somewhat similar spatial structure (correlations falling off as a function of distance), then the same function of average correlation versus distance could arise independent of the relative amplitude of the artefactual and genuine physiological signals. In fact our results show very long-range correlations for the brain, which are not present in the phantom data. These are likely to be caused by a combination of respiration, the cardiac rhythm and cognitive processes. A better characterization of the artefactual component might lead to correction techniques or incorporation of the artefactual effects into the statistical modeling.

Conclusion

Correlations between voxel time courses do not necessarily reflect brain processes. Instead, fMRI is affected by artefactual correlations, which are very strong for neighboring voxels and clearly present even at large distances. Such artefactual correlations could be caused by a wide range of factors (Fig. 4). This needs to be taken into account in the neuroscientific interpretation of voxel correlations. Future studies will need to assess the relative contribution of artefactual and genuinely physiological covarying processes to time-course correlations found in human fMRI data.

References

Bodurka, J. (1997) Field-cycling NMR relaxometry of molecular dynamics at biological interfaces in eye lenses: The Levy walk mechanism. *J. Chem Phys.* **107**, 5621-5624.

Büchel, C., Friston, K. J. (1997) Modulation of connectivity in visual pathways by attention: cortical interactions evaluated with structural equation modelling and fMRI. *Cereb Cortex* **7**, 768-78.

Cox, D. D. & Savoy, R. L. (2003) Functional magnetic resonance imaging (fMRI) "brain reading": detecting and classifying distributed patterns of fMRI activity in human visual cortex. *Neuroimage* **19**, 261-70.

Crank, J. (1975) *The mathematics of Diffusion.* London: Oxford University Press.

Einstein, A. (1956) *Investigations on the Theory of Brownian Movement.* New York Dover.

Farzaneh, F., Riederer, S. J., Pelc, N. J. (1990) Analysis of T2 limitations and off-resonance effects on spatial resolution and artifacts in echo-planar imaging. *Magnetic Resonance in Medicine* **14**, 123-139.

Fick, A. (1855) On liquid diffusion. *Philos Mag* **10**, 30-39.

Formisano, E., Esposito, F., Di Salle, F., Goebel, R. (2004) Cortex-based independent component analysis of fMRI time series. *Magn Reson Imaging* **22**, 1493-504.

Friston, K. J., Frith, C. D., Liddle, P. F., Frackowiak, R. S. Functional connectivity: the principal-component analysis of large (PET) data sets. (1993) *J Cereb Blood Flow Metab.* **13**, 5-14.

Friston, K. J., Worsley, K. J., Frackowiak, R. S. J., Mazziotta, J. C. & Evans, A. C. (1994) Assessing the significance of focal activations using their spatial extent. *Human Brain Mapping* **1**, 214-220.

Goelman, G. (2004) Radial correlation contrast — A functional connectivity MRI contrast to map changes in local neuronal communication. *NeuroImage* **23**, 1432– 1439.

Haxby, J. V., Gobbini, M. I., Furey, M. L., Ishai, A., Schouten, J. L. & Pietrini, P. (2001) Distributed and overlapping representations of faces and objects in ventral temporal cortex. *Science* **293**, 2425-30.

Kriegeskorte, N., Goebel, R., Bandettini, P. (2006) Information-based functional brain mapping. *Proc Natl Acad Sci U S A* **103**, 3863-3868.

Kriegeskorte, N., Bandettini, P. (2007). Analyzing for information, not activation, to exploit high-resolution fMRI. *NeuroImage*, in press.

McIntosh, A. R., Cabeza, R. E., Lobaugh, N. J. (1998) Analysis of neural interactions explains the activation of occipital cortex by an auditory stimulus. *J Neurophysiol.* **80**, 2790-6.

McKeown, M. J., Jung, T. P., Makeig, S., Brown, G., Kindermann, S. S., Lee, T. W., Sejnowski, T. J. (1998) Spatially independent activity patterns in functional MRI data during the stroop color-naming task. *Proc Natl Acad Sci U S A* **95**, 803–10.

Roebroeck, A., Formisano, E., Goebel, R. (2005) Mapping directed influence over the brain using Granger causality and fMRI. *NeuroImage* **25**, 230-42.

Schmitt, F., Stehling, M. K., Turner, R. (1998) *EPI Theory, Technique and Application.* Springer.

Worsley, K. J., Evans, A. C., Marrett, S., Neelin P. (1992) A three-dimensional statistical analysis for CBF activation studies in human brain. *J Cereb Blood Flow Metab.* **12**(6):900-18.

Zang, Y., Jiang, T., Lu, Y., He, Y., Tian, L. (2004) Regional homogeneity approach to fMRI data analysis. *NeuroImage* **22**, 394– 400.

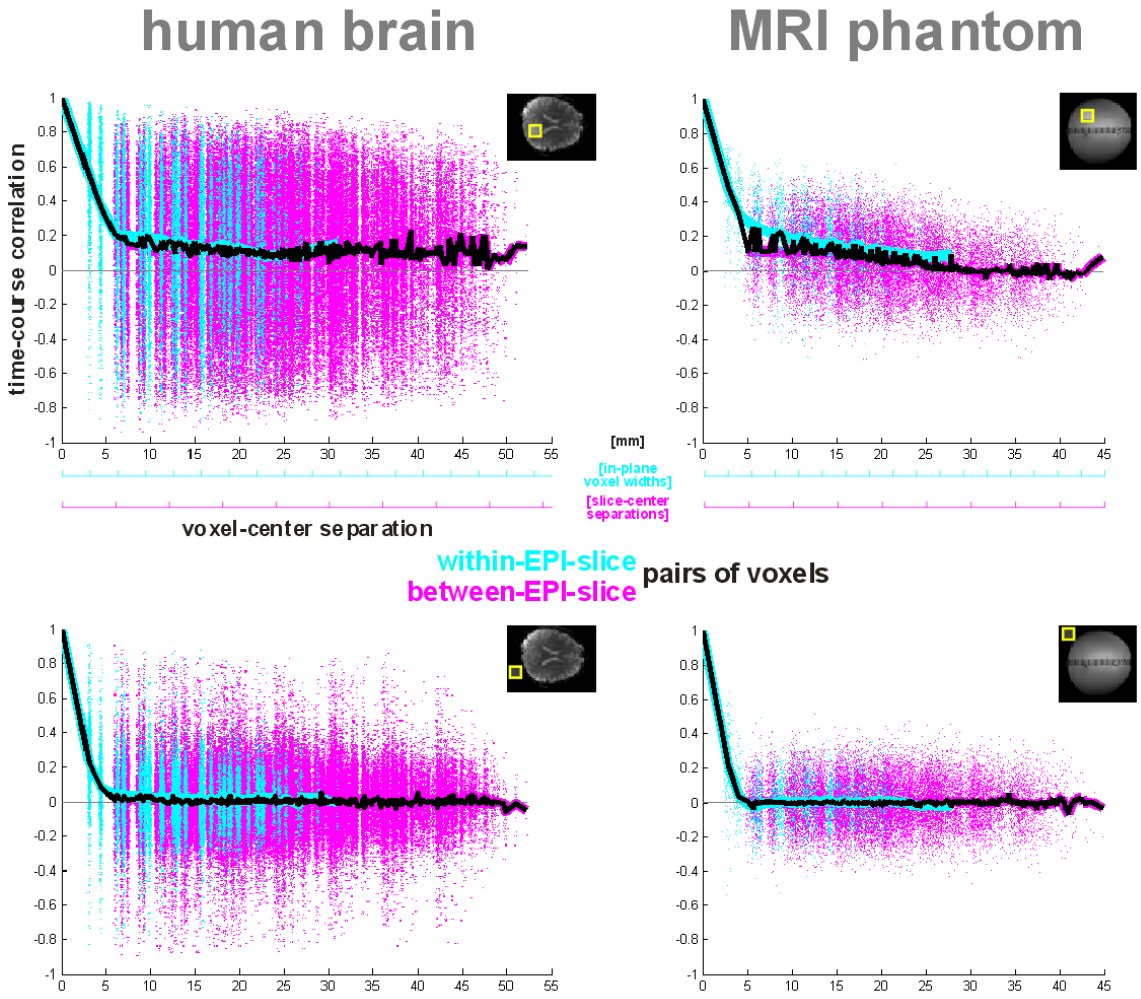

Fig. 1: **Short-range time-course correlation**. Linear correlation between the voxel time courses as a function of the distance between the voxels for the human brain in resting state (left) and an MRI phantom (right). Each pair of voxels is represented by a dot (cyan if the voxels are from the same slice, magenta otherwise). The average correlation functions are plotted as solid lines (black for all voxel pairs, cyan for within-slice voxel pairs, magenta for between-slice voxel pairs). These analyses were performed for cubic regions of interest (yellow squares) of 8×8×8 voxels located either inside the measured object (top) or outside of it (bottom). Note that we used these regions of interest to limit the number of pairwise correlations. However, results are not strongly dependent on the placement of the regions.

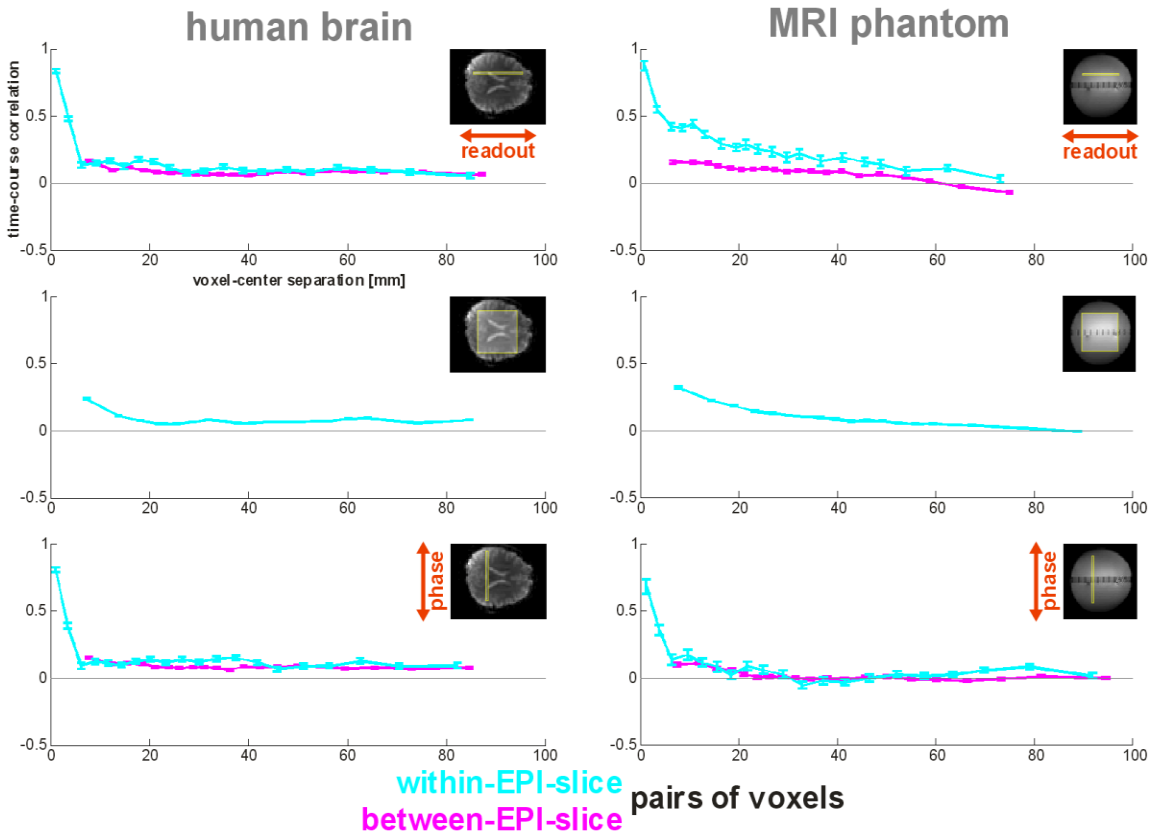

Fig. 2: **Long-range time-course correlation**. As Fig. 1, this figure shows the linear correlation between two voxels averaged across voxel pairs separated by the same distance. Here, however, the voxel separation (horizontal axes) goes up to about 8 cm (long-range) and the ROIs are slices (top: sagittal; middle: axial as measured, bottom: coronal). Averaging is performed separately for voxel pairs with both voxels residing in the same EPI (i.e. axial) slice (cyan) and for voxel pairs with voxels from different EPI slices (magenta). Data points have been grouped into 20 equally populated bins along the voxel-separation axis before averaging. Error bars indicate +/- 1 standard error of the mean. Note that even in the phantom (right column) the average voxel correlation can be clearly positive at voxel separations as high as 5 cm for voxels from different slices.

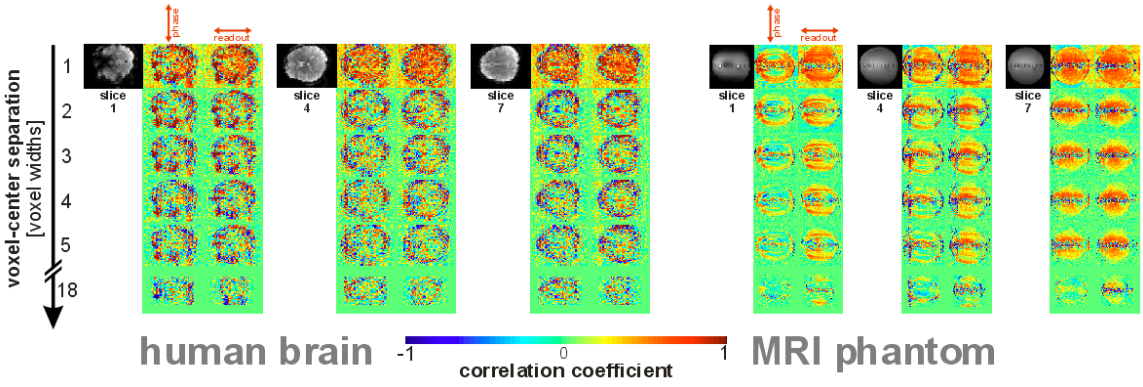

Fig. 3: **Spatial structure of time-course correlations**. For each pair of voxels separated by a given number of voxel widths either along the phase-encode or the readout direction within the same slice, we compute the linear correlation between time courses of the two voxels and store the correlation coefficient in a spatial map at the intermediate location between the two voxels.

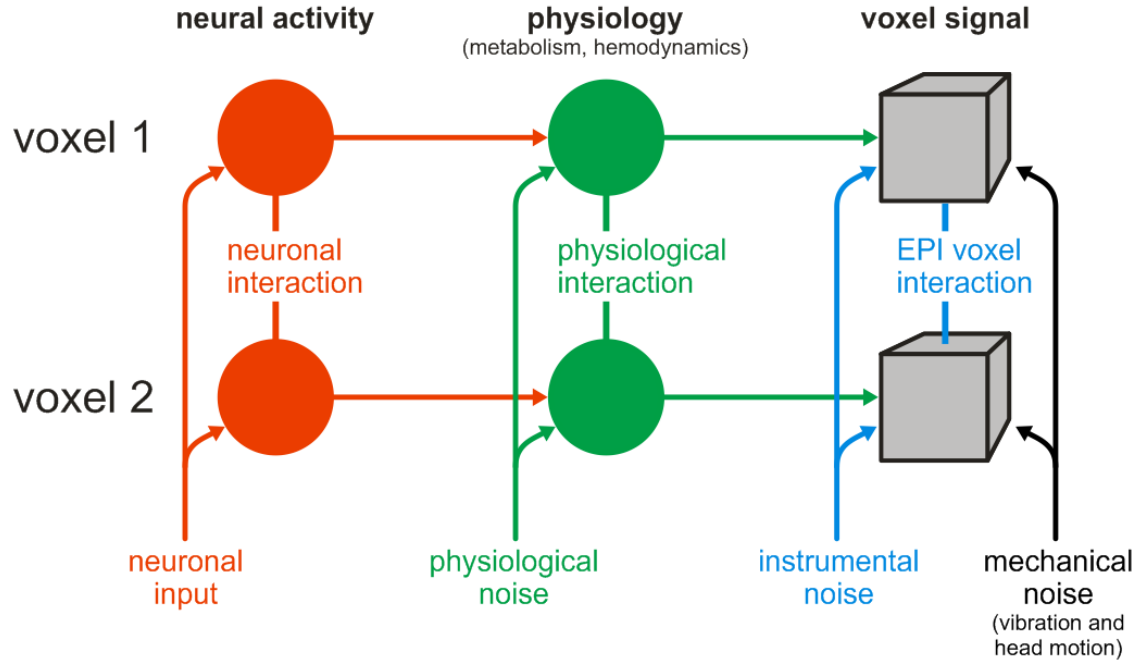

Fig. 4: Potential causes of correlations between fMRI voxel time courses. When two voxel time courses are found to be correlated, the cause could be neuronal (red). In particular, it could be a neuronal interaction or common neuronal input to the two sites.

However, a range of non-neuronal factors (green, blue, black) can also cause voxel correlation. These include (1) physiological factors (green), such as a physiological (e.g. hemodynamic) interaction between the two sites or a physiological noise source affecting both sites (e.g. the cardiac rhythm), (2) instrumental factors (blue), such as a common instrumental noise source or an interaction between the voxels due to MR physics and EPI image reconstruction, and finally (3) mechanical noise, for example vibration from the scanner gradients or the subject's head movements. The fact that fMRI voxel time-course correlations are observed even when a phantom is imaged (Figs. 1-3) indicates that there is a contribution of the non-neuronal factors to fMRI voxel correlations.